

Numerical analysis on various models of pressure snubbers in the hydrogen gas compressing system

Hyo Min Jeong¹, Han Shik Chung^{1,*}, Wanda Ali Akbar², Gyeong Hwan Lee²,
Kyu Jin Shim² and Yong Hun Lee²

¹*School of Mechanical and Aerospace Engineering, Gyeongsang National University, Institute of Marine Industry, Tongyeong, 650-160, Korea*

²*Graduate School, Department of Mechanical and Precision Engineering, Gyeongsang National University, 445 Inpyeong-dong, Tongyeong, 650-160, Korea*

(Manuscript Received January 31, 2007; Revised January 4, 2008; Accepted January 8, 2008)

Abstract

This paper explains about numerical modeling of gas flow passing through a snubber, pulsation damper, in a hydrogen gas compressor system. The verification of the preliminary model was done successfully by comparing it with experimental results. Numerical analysis for various snubber dimensions is the focus of this present study. Thirty models of snubber were created by varying snubber height and buffer angle, and then simulated with the real working condition of a hydrogen gas compressing system. The CFD code package used was a Star CD with transient analysis and $k-\varepsilon$ / high Reynolds number as the turbulence model. The study was done by comparing pressure loss and pressure pulsation, since these two parameters are the objective functions in snubber optimization. The best snubber is the one that has the minimum pressure loss and pressure pulsation. Numerical result shows that the pressure loss grows with the increment of snubber volume. To the contrary, however, the pressure pulsation is decreased. Determining the buffer angle as the adjusted variable, the minimum pressure loss occurred at 30° . But pressure pulsation trend was escalating.

Keywords: Hydrogen gas; Compressing system; Snubber; Pressure pulsation; CFD.

1. Introduction

The use of hydrogen as a transport fuel has been investigated for a number of decades, but in the past 10 years the number of research and pilot projects has escalated. This increased interest and investment has been stimulated by a perceived need to replace fossil fuels for environmental and/or security of supply reasons. The recent hikes in the price of oil have also added impetus to the movement towards hydrogen and other alternative fuels [1]. The main motivation of all research in the hydrogen energy development field is how to make it economically feasible to use. There are two approaches to minimize the production cost of hydrogen energy: a holistic approach and a

particular approach. The intention of the holistic approach is to find the most optimum process route from “well to wheel.” a methodology for the integrated production planning and reactive scheduling in the optimization of a hydrogen supply network like the one proposed [2]. Meanwhile the aim of the particular approach is improving separately each process of the hydrogen production chain.

The compressing system plays an important role in the whole system, because its function is to increase the gas pressure, which is very important for transferring and storing the hydrogen gas. The hydrogen compressor used was a positive-displacement reciprocating type. A schematic drawing of the hydrogen compressing system is shown by Fig. 1. From that figure, the snubbers applied to each compressor stage can be seen clearly. There, four snubber units are used

*Corresponding author. Tel.: +82 55 640 3185, Fax.: +82 55 640 3188

E-mail address: hschung@gnu.ac.kr

DOI 10.1007/s12206-008-0104-7

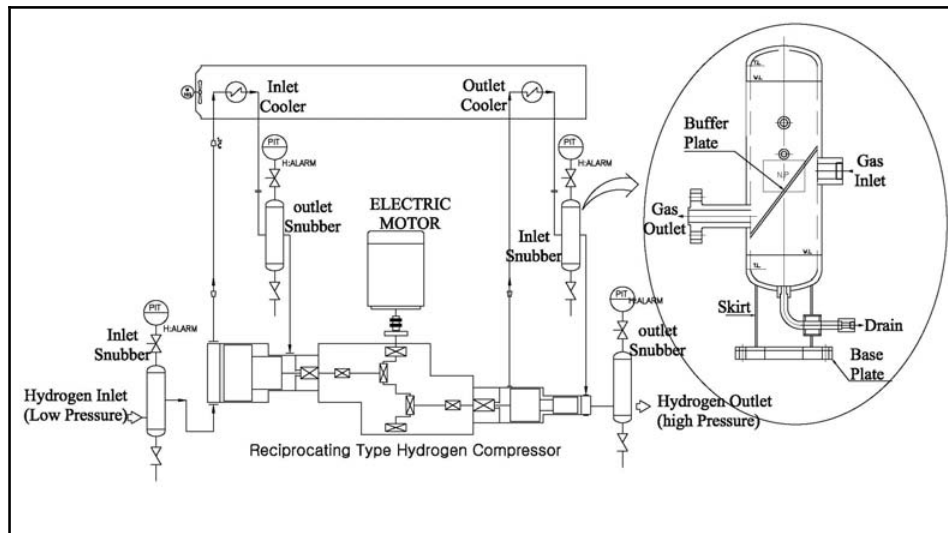


Fig. 1. Schematic drawing of a hydrogen gas compressing system.

for each inlet and outlet at the first and second stage. A positive-displacement compressor produces pressure pulsations due to their cyclic operation. The analysis of pressure pulsations in the exhaust pipe is important for various reasons: they directly affect the quantity of energy required for medium compression due to dynamic pressure charging, or inversely, dynamic suppression of suction and discharge processes; they cause mechanical vibrations of a compressed gas piping network; they cause aerodynamic and mechanical noise; they affect the dynamics of working valves in valve compressors, and they intensify the process of heat convection in the heat exchangers in the gas network [3]. Other researches about the presence of fluctuating pressure and its effect have been published [4] and [5]. More details about pressure pulsation, especially its flow and propagation characteristics, are discussed [5] and [6].

In order to restrain the manufacture of snubbers, one should consider the design of pulsation and vibration control for hydrogen compressor system requirements in the API Standard 618 book [7]. There is written the basic means used to control detrimental pulsations and vibrations. They are: (1) pulsation suppression devices such as pulsation filters and attenuators (including those of proprietary commercial designs based on acoustical suppression techniques), volume bottles without internals, choke tubes, orifice systems, and selected piping configurations; (2) system design based on studies of the interactive effects

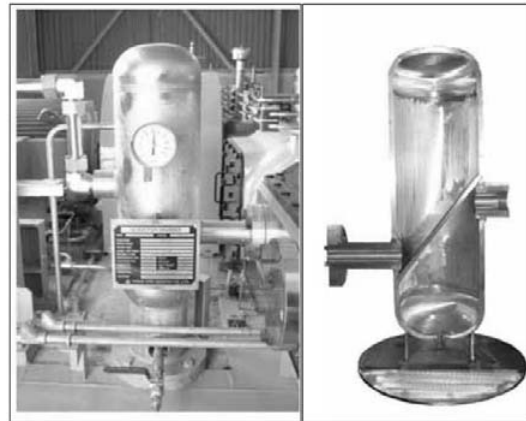


Fig. 2. Detailed and cut-away view of a snubber.

of pulsations and the attenuation requirements for satisfactory piping vibration, compressor performance, and valve life; and (3) mechanical restraints such as type, location, and number of pipe hold-downs.

Based on that guidance a snubber is designed and used. Moreover, in order to enhance the damper performance due to pressure pulsation, a flat plate, called a buffer, is inserted inside the snubber. The installation of a buffer inside a snubber can be seen in the cut-away view shown schematically in Fig. 1 and in actuality in Fig. 2 (the right side figure). An experiment to find the effect of buffer presence in a snubber was conducted [8]. This resulted in the fact that a snubber with a buffer has better performance.

For several parameters in the low pressure range,

hydrogen gas has the same character with atmospheric air. Especially, to observe the pressure from a physical approach (without considering the chemical character), pressured air can be used to represent hydrogen gas. Modeling a hydrogen compressor by using an air compressor unit brought a good agreement with the CFD simulation. After that, the study was focused on numerical analysis to achieve the optimum dimension for a snubber. This paper explains the effect of varying buffer angle to the pressure characteristics. They are pressure loss and pressure pulsation. Three model groups, distinguished by the volume, are compared.

2. Mathematical formulation

The purpose of deriving a mathematical model in CFD is to find the appropriate relation between each fluid flow property. The transient, three dimensional, compressible, turbulent flow of the gas in the test problems is governed by partial differential equations that express the principles of conservation of mass and momentum. Since temperature analyses were not included in this study, therefore the energy conservation equation was not used. In this paper, the turbulent model chosen was *k-ε* with high Reynolds number.

2.1 The continuity and momentum equation

The concept of mass conservation or continuity equation is balanced between incoming, outgoing and changing of mass in a control volume. This can be written in a mathematical expression as stated below.

$$\frac{\partial \rho}{\partial t} + \frac{\partial(\rho u_i)}{\partial x_i} = s_m \tag{1}$$

where x_i , u_i , $i=1,2,3$, ρ , t , and s_m are the Cartesian coordinates, the Cartesian velocity components, the density of fluid, time and mass source, respectively.

For momentum balance analysis, the momentum equation is used. The general form of this second concept can be written in:

$$\frac{\partial(\rho u_i)}{\partial t} + \frac{\partial(\rho u_i u_j - \tau_{ij})}{\partial x_j} = -\frac{\partial p}{\partial x_i} + s_i \tag{2}$$

where p and s_i are the pressure and momentum source component. And stress tensor component τ_{ij} is described as

$$\tau_{ij} = 2\mu s_{ij} - \frac{2}{3}\mu \frac{\partial u_k}{\partial x_k} \delta_{ij} - \overline{\rho u_i u_j} \tag{3}$$

where μ and δ_{ij} are the fluid viscosity and the Kronecker delta, is unity when $i = j$ and zero otherwise, respectively. The rate of strain tensor s_{ij} is given by

$$s_{ij} = \frac{1}{2} \left(\frac{\partial u_i}{\partial x_j} + \frac{\partial u_j}{\partial x_i} \right) \tag{4}$$

2.2 Turbulence model

One of the most important decisions in computational fluid dynamics is the choice of an appropriate turbulence model. The principal goal of any turbulence model is to provide a method for calculating the influence of turbulence fluctuations on the mean flow field. In this study, observation was proposed to get the fluid flow general characteristics inside the closed channel. Therefore, the *k-ε* model of turbulence was chosen to represent the turbulence effect in this study. The turbulent kinetic energy balance can be written as the following equation:

$$\begin{aligned} \frac{\partial(\rho k)}{\partial t} + \frac{\partial}{\partial x_j} \left[\rho u_j k \left(\mu + \frac{\mu_t}{\sigma_k} \right) \frac{\partial k}{\partial x_j} \right] \\ = \mu_t (P + P_B) - \rho \varepsilon - \frac{2}{3} \left(\mu_t \frac{\partial u_i}{\partial x_i} + \rho k \right) \frac{\partial u_i}{\partial x_i} + \mu_t P_{NL} \end{aligned} \tag{5}$$

where k and ε are the turbulence kinetic energy and the turbulence dissipation rate, respectively.

In the equation above P , P_B and P_{NL} are defined as

$$P \equiv S_{ij} \frac{\partial u_i}{\partial x_j} \quad \text{and} \quad P_B \equiv -\frac{g_i}{\sigma_{h,t}} \frac{1}{\rho} \frac{\partial \rho}{\partial x_i} \tag{6 and 7}$$

$$P_{NL} = \frac{\rho}{\mu_t} \overline{u_i u_j} \frac{\partial u_i}{\partial x_j} - \left[P - \frac{2}{3} \left(\frac{\partial u_i}{\partial x_i} + \frac{\rho k}{\mu_t} \right) \frac{\partial u_i}{\partial x_i} \right] \tag{8}$$

and the turbulence viscosity μ_t is shown as

$$\mu_t = f_\mu \frac{C_\mu \rho k^2}{\varepsilon} \tag{9}$$

Meanwhile, the turbulent dissipation rate balance obeys the following equation:

$$\begin{aligned} & \frac{\partial(\rho \varepsilon)}{\partial t} + \frac{\partial}{\partial x_j} \left[\rho u_j \varepsilon - \left(\mu + \frac{\mu_t}{\sigma_\varepsilon} \right) \frac{\partial \varepsilon}{\partial x_j} \right] \\ &= C_{\varepsilon 1} \frac{\varepsilon}{k} \left[\mu P - \frac{2}{3} \left(\mu_t \frac{\partial u_i}{\partial x_i} + \rho k \right) \frac{\partial u_i}{\partial x_i} \right] \\ &+ C_{\varepsilon 3} \frac{\varepsilon}{k} \mu_t P_b - C_{\varepsilon 2} \frac{\varepsilon^2}{k} + C_{\varepsilon 4} \rho \varepsilon \frac{\partial u_i}{\partial x_i} + C_{\varepsilon 1} \frac{\varepsilon}{k} \mu_t P_M \end{aligned} \quad (10)$$

and all of the coefficients whose values are written as $C_{\varepsilon 1}=1.44; C_{\varepsilon 2}=1.92; C_{\varepsilon 3}=1.44; \sigma_\varepsilon=1.22; \sigma_k=1.0; C_\mu=0.09$.

2.3 Pressure characteristics analysis

The main functions of the snubber are to reduce the pulsation and (at the same time) to maintain the pressure magnitude [8]. For that reason, the three following equations are derived:

$$\begin{aligned} \Delta P &= P_{in} - P_{out}, \quad P_{TL} = \frac{\Delta P}{P_{in}} \times 100\% \quad \text{and} \\ P_F &= \sum \frac{\Delta P}{2 \times P_{mean}} \times 100\% \end{aligned} \quad (11, 12 \text{ and } 13)$$

In these equations, P_{mean} , ΔP , P_{in} , P_{out} , P_{TL} , P_F and are pressure difference, inlet pressure, outlet pressure, total pressure loss, pressure pulsation and mean pressure value, respectively. Reducing the pulsation means reducing P_F value, while keeping the pressure magnitude means keeping the P_{TL} value as low as possible.

3. Numerical validation

The computational code used was Star CD (Version 3.24) [9], which solved the full 3D time dependent Navier-Stokes, continuity and energy equations using the finite volume method. This commercial code is widely used in the numerical simulation of different flow conditions in various complex geometries and was chosen in this study because of its proven capability and validity. The turbulent flow in this investigation is considered to be transient, incompressible, viscous, Newtonian and isotropic.

The numerical solution involves splitting the geometry into many sub-volumes and then integrating the differential equations over these volumes to produce a set of coupled algebraic equations for the velocity components, and the pressure at the center of each volume. The solver guesses the pressure field and then solves the discretized form of the momen-

tum equations to find new values of the pressure and velocity components. This process continues, in iterative manner, until the convergence criterion is satisfied. In this study, simulation was started by verifying the numerical result with the experimental result. This was done and gave good agreement. Afterward, a simulation series for different snubber models was conducted.

3.1 Modeling and grid system

The model used for validation was made with dimensions shown in Fig. 3. The geometry was drawn by using a CAD commercial software package and then imported to pro-Surf (Star CD’s surface mesh generator) as an Initial Graphics Exchange Specification file (IGES). The surface mesh file was generated by using pro-Surf and the triangular surface mesh file was then transferred to pro-am (Star CD’s volume mesh generator) to create the trimmed hexahedral cell volume mesh for the model. In order to reduce the cell number so the calculation work was also reduced, the model was built in a one-half type, and then the symmetry boundary condition was applied on the cutting plane. This is regarding the symmetrical shape of the snubber. The computational mesh consists of about 50,000 trimmed hexahedral cells.

3.2 Boundary condition

In order to solve the partial differential equations described in section 2, appropriate boundary conditions must be declared for all boundaries of the computational domain. The boundary conditions associated with the computational domain are inflow, outflow and symmetry plane.

The inflow was set to the pressure value taken from measured data form the experiment. The data is tran-

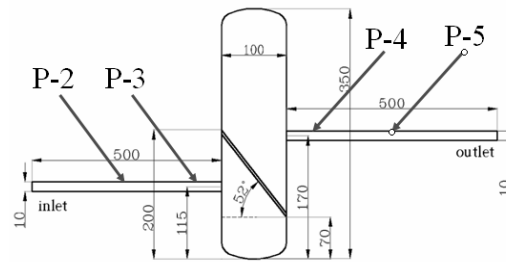


Fig. 3. Dimension of computational model with observed points positions.

sient and waving within the maximum and minimum limit. The pressure value is different for each motor frequency. Fig. 4 shows the inflow data as the boundary condition for motor frequency 20, 40 and 60 Hz. The boundary condition for the outflow was set to the atmospheric pressure value, 101.325 kPa. The dimension of the model is depicted in Fig. 3. In this figure the four points where the sensors were placed also are pointed out. So the corresponding location in the CFD model must be the observing objects.

3.3 Verification of the computational method

The simulation was run for three simulations, ac-

ording to different motor frequency. During the simulation running, pressures at the measuring points were recorded. From the data acquired, the graph was plotted as Fig. 5. All of those graphs show the same trend between CFD and the experimental result. Then the mean pressures of each case were compared as in Fig. 6. There can be seen the pressure drop with the increasing distance from the compressor and also lowering the motor frequency. To measure the difference between those data, a difference ratio should be calculated. Then, good agreement can be said regarding the relatively small difference ratio with a maximum of only 0.55 %. Fig. 7 shows the difference ratio between CFD and experimental data.

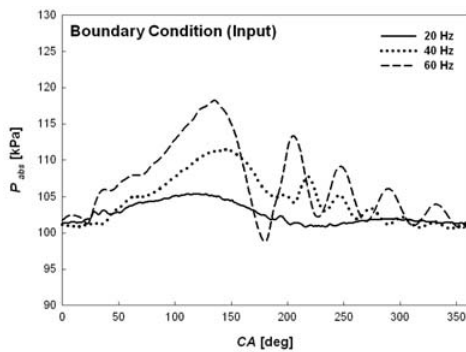


Fig. 4. Inlet boundary condition for numerical simulation.

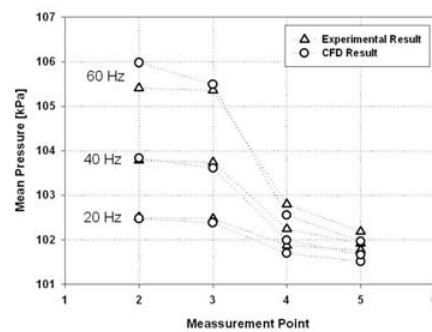


Fig. 6. Mean pressure value for each motor frequency: 20 Hz, 40 Hz and 60 Hz.

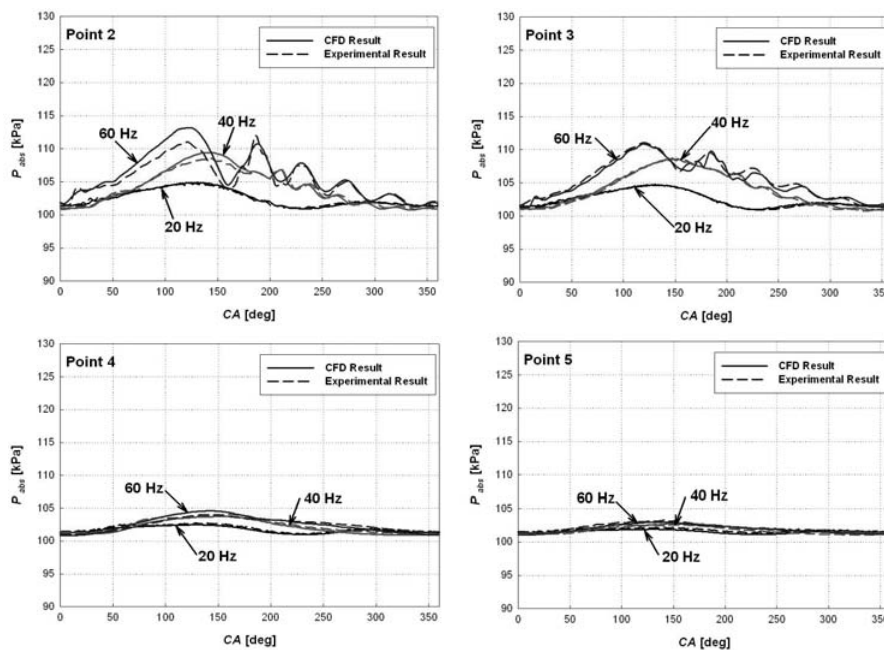


Fig. 5. CFD and experimental result at each point.

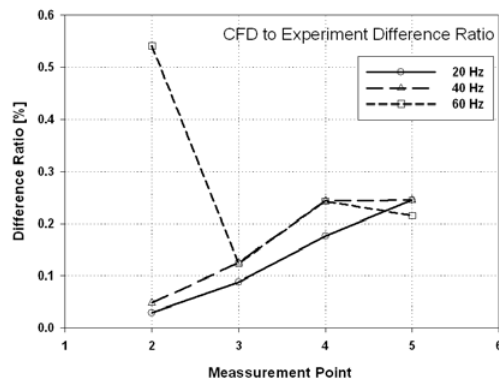


Fig. 7. CFD to experiment difference ratio.

4. Numerical analysis

The appropriate modeling and simulation setting described in the previous discussion are the basis for extending the investigation for various dimensions of snubber. The purpose is to find its optimum design. In designing a snubber several dimensions such as snubber height (H), snubber diameter (D), buffer width (W) and buffer angle (θ) must be defined. Fig. 8 illustrates all of the geometrical variables mentioned above and also the monitoring points (P-1 and P-2). Each model requires a specific grid system as shown in Fig. 9. Like the simulation to get verified data, a trimmed-hexagonal cell also was used. The half-symmetry model was used to reduce the cell number. Therefore, the calculation job would be reduced. Special treatment of meshing was applied to the area near the wall. In these areas the mesh size was made much smaller, so accurate calculations could be made. Fig. 9 (the right side figure) shows the detailed cross section of the model.

The objective of this work was to solve real problems occurring in a hydrogen gas station. Therefore, in this simulation real dimensions and conditions were used. The model with $H/D = 3.82$ with 0.0147 mm^3 is the one which is used in industry; in this paper this is referred to as the standard model. Two other models were studied as the benchmarks to get the parameter trend based on varying volume. One model taken had a bigger volume than the standard model and the other had smaller one than the standard. The simulation run in this paper occupied three groups of snubber volume: $H/D = 3.23$, $H/D = 3.82$ and $H/D = 4.41$. The volume size for each model was 0.0124 mm^3 , 0.0147 mm^3 and 0.0170 mm^3 respectively. The complete dimension parameters are listed in Table 1.

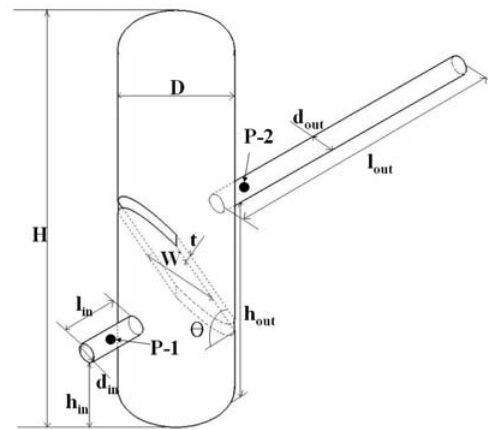


Fig. 8. Model Geometry and monitoring point positions.

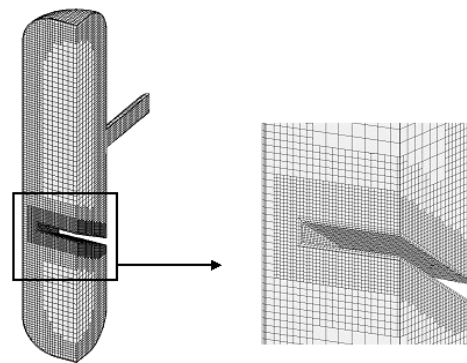


Fig. 9. Grid system of the models.

To produce a comparable result to the real condition, so the boundary condition, material properties and numerical setting were adjusted to approach reality. The inlet pressure for the boundary condition was set to a high enough value representing the operational pressure in a real hydrogen gas plant. This mean pressure value was 10 MPa with pulsation factor of 2 MPa. Fig. 10 shows this inlet boundary condition. On the other hand, the pressure outlet boundary condition was set at steady 10 MPa. Hydrogen gas properties applied into this computation were taken from the Star CD material database. The computation was set with transient condition, compressible flow and using a $k-\varepsilon$ high Reynolds number turbulent model. Upwind scheme was chosen to execute the calculation for all variables, such as mass, U , V , W momentum, pressure and turbulent kinetic energy.

The study was focused on pressure at point 1 and point 2 as the monitoring points. These points, both at inlet and outlet pipe, are located 50 mm from the

Table 1. Geometrical data for various snubber models.

Parameters (mm)	H/D 3.23	H/D 3.82	H/D 4.41
Body diameter, D	170		
Body height, H	550	650	750
Inlet pipe diameter, d_{in}	30		
Outlet pipe diameter, d_{out}	30		
Inlet pipe length, l_{in}	100		
Outlet pipe length, l_{out}	500		
Inlet pipe position form bottom, h_{in}	175		
Outlet pipe position form bottom, h_{out}	310		
Buffer width, W	60		
Buffer thickness, t	10		
Buffer angle, θ	10°-50° (increase with 5°)		
Volume (m ³)	0.0124	0.0147	0.0170
Grid cells number	65,000	75,000	85,000

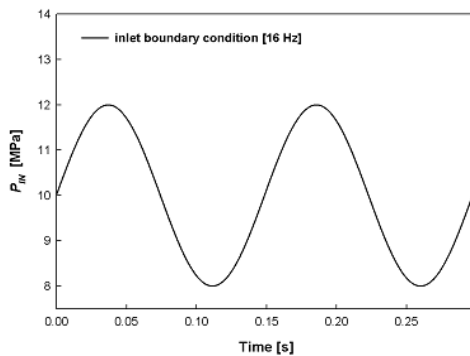


Fig. 10. Inlet boundary condition.

snubber wall. These points were chosen in order to analyze damping phenomena inside the snubber.

5. Results and discussion

The simulation produced the mean pressure values at point 1 and point 2. The mean pressure at point 1 is shown by Fig. 11, meanwhile at point 2 by Fig. 12. At point 1, inlet pipe, the mean pressure decreased with the increasing snubber volume. For all snubber volume models, the trends are quite similar based on varying buffer angle. For H/D = 3.23, starting from 10 deg up to 30 deg, the pressure was quite constant. Then it started to increase when $\theta = 30$ deg until 50 deg. For H/D = 3.82, starting from 10 deg up to 35 deg, the pressure was quite constant. Then it started to

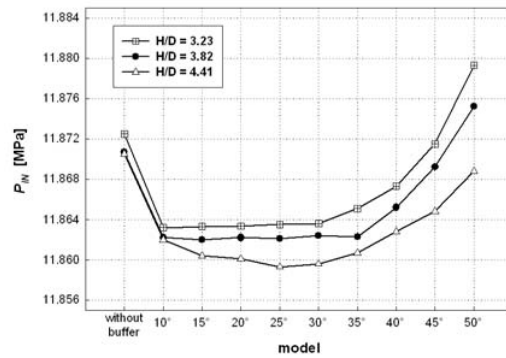


Fig. 11. Mean pressure at point 1.

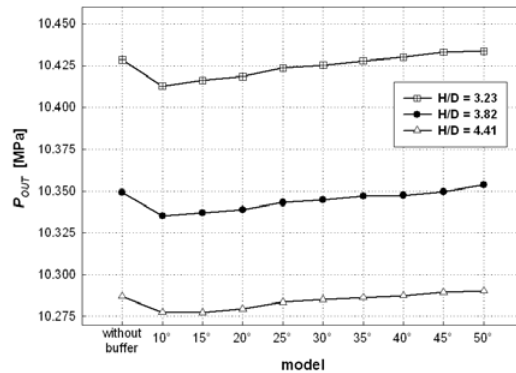


Fig. 12. Mean Pressure at point 2.

increase when $\theta = 35$ deg until 50 deg. The uniqueness occurred in H/D = 4.41, the pressure declined from 10 deg until 25 deg and smoothly inclined from 25 deg until 35 deg then drastically inclined from 35 deg to 50 deg. Pressure without buffer is bigger than pressure with 45 deg buffer for all models. At point 2, outlet pipe, the mean pressure also indicates a unique pattern. All models show smooth increasing from 10 deg until 50 deg.

Applying Eq. 12 and 13, Fig. 13 and Fig. 14 can be made. These two graphs depict the objective functions. As known before, P_{TL} and P_F are the pressure characteristics which become the optimization parameters. The goal of this optimization was to minimize both of those values. As can be seen in Fig. 13, P_{TL} is increasing with increasing snubber volume. All models show a curved-like trend with minimum value at 35 deg. For H/D = 3.82 and H/D = 4.41, the value declines smoothly starting from 10 deg until 35 deg, after that inclining with very small changes. And for H/D = 3.23, the value decline smoothly starts from 10 deg until 40 deg, after that inclining up to 50 deg.

Fig. 14 shows phenomena similar with Fig. 12. The

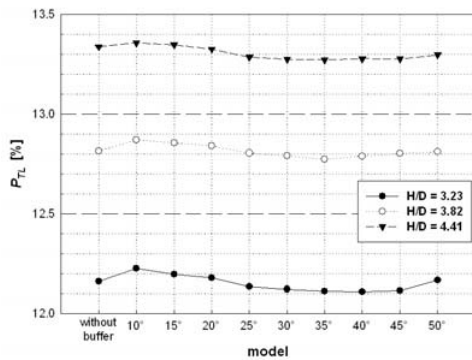


Fig. 13. Pressure loss variation.

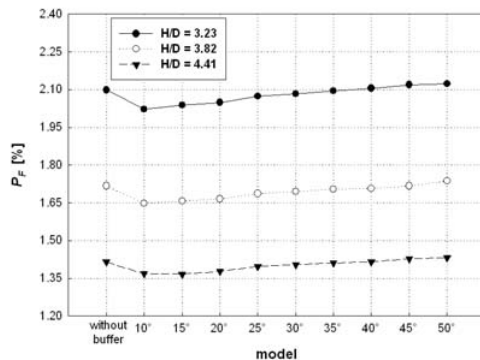


Fig. 14. Pressure pulsation variation.

P_F is increasing from 10 deg until 50 deg for all models. According to the fact discussed above, the optimization faces a problem where the minimum value for both parameters does not occur at the same buffer angle. Therefore, an advance study to determine the optimum value must be developed. This should consider not only minimizing mean pressure loss and pressure pulsation but also minimizing the snubber volume.

6. Conclusions

The present study has shown that computational fluid dynamics (CFD) can be applied to study pressure characteristics through a snubber. The numerical analysis on the snubber has been done and given information that can be summarized as follows:

The objective in optimizing a snubber dimension is to make the mean pressure loss and pressure pulsation as minimum as possible. In this case, consideration of the points stated by the API is a necessity.

A simulation using CFD commercial code with described numerical setting can result in a good repre-

sentation of real conditions. This is proved by the very small difference ratio, which value is not more than 0.55 %.

The mean pressure both at inlet and outlet pipe shows a unique characteristic shown by Figs. 11 and 12. At point 1 and point 2 the mean pressure is decreasing with increment of the snubber volume size. Generally, the mean pressure is increasing when buffer angle is added.

The pressure loss grows when snubber volume size is enlarged. Regarding the varying buffer angle, the minimum value of mean pressure loss P_{TL} occurs when buffer angle is about $\theta = 35^\circ$. Decreasing or increasing the buffer angle will increase the mean pressure loss P_{TL} .

The pressure pulsation drops when snubber volume size is enlarged. By varying the buffer angle, the minimum value of pressure pulsation P_F in this study occurred when buffer angle $\theta = 10^\circ$. Increasing the buffer angle will increase pressure pulsation P_F .

Acknowledgments

This research was financially supported by the Ministry of Commerce Industry and Energy(MOCIE) and Korea Industrial Technology Foundation(KOTEF) through the Human Resource Training Project for Regional Innovation and the second-phase of the Brain Korea 21 project.

References

- [1] S. Shayegan, D. Hart, P. Pearson and D. Joffe, Analysis of the cost of hydrogen infrastructure for buses in London, *Journal of Power Sources*, Elsevier (2006).
- [2] S. A. Heever, and I. E. Grossman, A strategy for the integration of production planning and reactive scheduling in the optimization of hydrogen supply network, *Journal of Computers and Chemical Engineering*, 27 (2003) 1831-1839.
- [3] P. Cyklis, Experimental Identification of the Transmittance Matrix for any Element of the Pulsating Gas Manifold, *Journal of Sound and Vibration* 244 (5) (2000) 859-870.
- [4] S. I. Seo, C. S. Park and O. K. Min, A Study on Fluctuating Pressure Load on High Speed Train Passing through Tunnels, *Journal of Mechanical Science and Technology (KSME Int. J.)*, 20 (4) (2006) 482-493.

- [5] H. G. Lee, H. C. Sohn, H. N. Lee and G. M. Park, An experimental study on flow characteristics of turbulent pulsating flow in a curved duct by using LDV, *Transactions of the KSME B*, 25 (11) (2001) 1561-1568.
- [6] Y. T. Yoo, G. D. Na and J. H. Kim, Propagation characteristics of pressure pulse of unsteady flow in a hydraulic pipeline, *Transactions of the KSME B*, 26 (2002) 1-11.
- [7] American Petroleum Institute (API), Reciprocating Compressor for Petroleum, Chemical, and Gas Industry Services, API Standard 618, 4th edition, Washington, (1995).
- [8] W. A. Akbar, K. J. Shim, and C. S. Yi, Gas pressure fluctuation characteristics inside pipe line passing through a snubber for hydrogen gas compressor, *Proceeding of Int. Conf. on Sustainable Energy Technologies*, Vicenza, Italy (2006).
- [9] CD Adapco Group, Methodology Star CD Version 3.24. (2004).